Pure appl. geophys. 152 (1998) 75–89
0033–4553/98/010075–15 $ 1.50 + 0.20/0

Pure and Applied Geophysics

Fault Lengths During the Patras 1993 Earthquake Sequence as Estimated from the Pulse Width of Initial *P* Wave

G-Akis Tselentis[1]

Abstract—The pulse width of the initial *P* wave was measured for three clusters of the aftershock sequence of the Patras (5.4 M_S) July 1993 earthquake. The data set consists of pulse width measurements of 250 microearthquakes recorded at a low-noise station of the University of Patras Seismological Network between 4-7-1993 and 1-8-1993. The statistical relation between the fault length and the earthquake magnitude was established for each one of the three clusters and is compared with other published relations. The relation also, between seismic moment and fault length was examined and showed a dependence upon the prevailing tectonic regime.

Key words: Pulse width, source length.

1. Introduction

Usually, earthquake source parameters are estimated using spectral techniques; the corner frequency is related to a source dimension through scaling laws that make assumptions about source geometry and rupture velocity, and the seismic moment is evaluated from the long-period spectral level (i.e., Brune, 1970). This conventional method however is not highly efficient when we deal with a large number of earthquakes, as in the present case.

An alternative approach is based on the measured pulse width of the initial *P* wave at an observation station of far-field. Pulse width methods, like spectral methods, do not require precise measurement of pulse amplitudes or instrumental response. Unlike spectral methods, though, the pusle width methods only require a very short part of the first arriving signal, which is relatively free of other interfering waveforms such as reflection, scattering, or multiple travel paths (Wu and Lees, 1996). In order to make accurate spectrum estimates, spectral methods typically use 0.5 to 2 sec of data, whereas the pulse width may be estimated over half a wavelength of the *P*-wave arrival.

O'Neill and Healy (1973) proposed such an approach for a spherical source. Frankel (1981) applied this method for an expanding circular crack. Frankel and Kanamori (1983) extended the initial *P*-wave pulse width method by

[1] University of Patras, Seismological Laboratory, Rio 261 10, Greece; tselenti@upatras.gr

incorporating a method of accounting for the seismograph site response, suggesting that for each seismograph site there was a "pulse width floor", a magnitude level below which the pulse width no longer decreased. OHTAKE (1986) extended the method to bilateral and unilateral propagation of rectangular faults. O'NEILL (1984) applied a similar methodology to derive source dimensions of small earthquakes at Parkfield. TSELENTIS *et al.* (1987) used the pulse width method to assess source dimensions of the Kalamata 1986 (S. Greece), aftershock sequence. Recently, ZUCCA *et al.* (1994) and WU and LEES (1996) employed pulse widths to investigate the attenuation characteristics of geothermal fields.

The purpose of the present study is to establish the statistical relation between the fault dimension L and earthquake local magnitude for small-sized earthquakes for the aftershock sequence of the Patras 1993 earthquake.

2. Theory and Method

Seismic sources are usually modeled as step dislocations on a fault plane, producing an impulsive displacement at the recording site.

First, we will derive the relation between the average pulse width of the initial P wave at a far-field station and the source duration time for the three types of faulting; bilateral, unilateral and expanding circular crack.

For the case of uni- and bi-lateral faulting it is assumed that the rupture occurs simultaneously over the entire width of the fault and that the fault length L is substantially larger than the fault width N, thus neglecting the contribution of the fault width.

For the case of bilateral rupture of a rectangular fault on which the rupture initiates at $x = a$ (Fig. 1), the pulse width of displacement at the observation station is calculated from simple physics as (OHTAKE, 1986):

$$T(L, \vartheta) = \frac{1}{L}\int_0^l \left\{\frac{(L-a)(k+\cos\vartheta)}{V_p}\right\} dl + \int_l^L \frac{a(k+\cos\vartheta)}{V_p}\, da$$

$$= \frac{L}{8kV_p}(6k^2 + 1 + \cos 2\vartheta) \tag{1}$$

where L is the fault length, θ is the angle between the station and rupture direction, V_p is the P-wave velocity, $k = V_p/V_r$ is the ratio of P wave to rupture velocity and l is given by

$$l = \frac{L}{2}\left(1 - \frac{\cos\vartheta}{k}\right). \tag{2}$$

Averaging over θ we obtain

$$T(L) = \int_0^{\pi/2} T(L, \vartheta)\sin\vartheta \, d\vartheta = \frac{L}{12kV_p}(9k^2 + 1). \tag{3}$$

Similarly, for the unilateral fault we obtain

$$T(L) = \frac{L}{V_p}k \tag{4}$$

and for a circular crack with diameter L

$$T(L) = \frac{L}{2V_p}\left(k + \frac{\pi}{4}\right). \tag{5}$$

Assuming $V_p = 5.5$ km/s and $k = 2.0$, the average pulse width is expressed by

$$\begin{aligned} T(L) &= 0.25\,L \ \text{(circular crack)} \\ &\quad 0.28\,L \ \text{(bilateral fault)} \\ &\quad 0.36\,L \ \text{(unilateral fault).} \end{aligned} \tag{6}$$

Obviously, the observed pulse width T_{obs} can be expressed as a linear combination of the intrinsic pulse width T and a correction term $c(R)$ which describes the path effect and depends on the hypocentral distance R as follows:

$$T_{\text{obs}}(L, \theta, V_p, r) = T(L, \theta, V_p) + c(R). \tag{7}$$

The correction term can be easily assessed by the pulse width of very small earthquakes for which T is expected to be negligibly small (FRANKEL and KANAMORI, 1983; OHTAKE, 1986). Effects of site and instrument are also incorporated in this correction term but it is not necessary to consider the station dependence since we use the data from the same seismometer at the same observation station.

3. Instrumentation and Data Processing

Data used in this work were recorded by station PAP of Patras University short-period seismic network (hereafter PATNET). The network consists of 17 stations, all of them equipped with a vertical component Teledyne S13 (1 Hz), seismometer operating with 60 dB amplification, filter with a band-pass filter at 0.2–50 Hz and in a low-noise environment.

Station PAP, which is used for measuring initial pulse widths in the present investigation, is one of the quietest stations of the network installed on a limestone outcrop, distant from any cultural source of noise. The seismometer has been positioned within a specially excavated shaft within the rock at a depth of 3 m and isolated from the environment by layers of volcanic ash and polyurethane.

The signals from the seismometers are radio-telemetered via FM subcarriers to the central recording site at the Seismological Laboratory of the University of Patras (base station), where a three-component seismometer station is deployed, in real time. There, they are anti-alias filtered with a 200-Hz analogue Butterworth low-pass filter, sampled at 100 Hz and converted to digital form with a resolution of 16 bits.

For the initial phase picking and data processing, SISMWIN (TSELENTIS *et al.*, 1994) an in-house developed software is used. SISMWIN employs features that are particularly convenient for arrival picking, zooming and noise reduction such as neural algorithms for *P*- and *S*-phase automatic picking, noise corrected deconvolved displacement seismograms, etc. Thus for seismograms with S/N ratio greater than 5, *P*- and *S*-wave arrival times are read with an accuracy of approximately 0.02 and 0.05 s, respectively.

For the event location and magnitude calculation the HYPO71PC (LEE and VALDES, 1985) is used. The best velocity model was obtained using all well-recorded (clear *P* and *S* arrivals) events by at least six stations. The final velocity model used for the area of Patras is shown in Table 1.

The magnitude which is reported for all the events is the local magnitude M_L calculated from the total signal duration. The computation was also done by

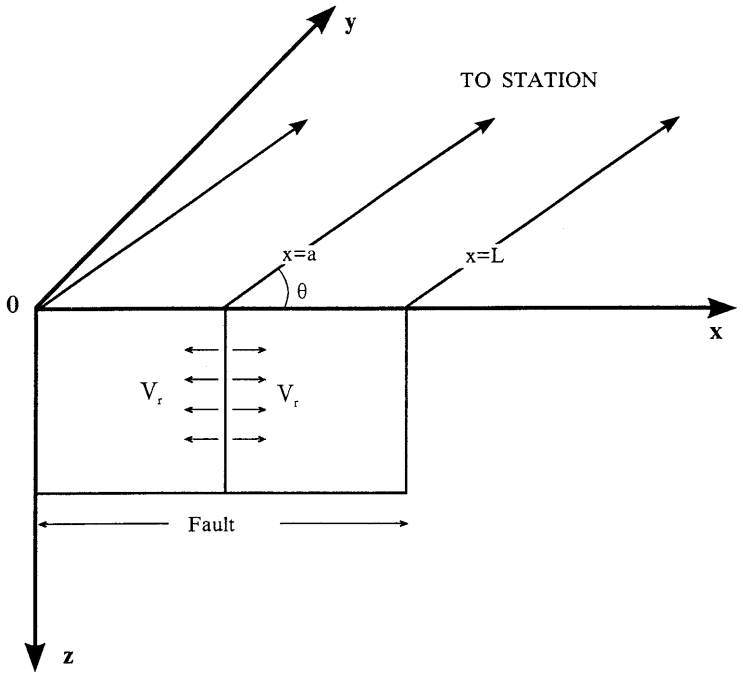

Figure 1
Simplified geometry of bilateral faulting.

Table 1

The P and S velocity model used for final event location

Depth (km)	V_p (km/s)	V_s (km/s)
0	1.42	0.80
0.5	2.67	1.50
1	4.45	2.50
2	5.7	3.20
5	6.0	3.37
18	6.4	3.60
39	7.9	4.44

HYPO71PC using the formula defined by LEE *et al.* (1972) in conjunction with the one described in KIRATZI and PAPAZACHOS (1985) and MELIS *et al.* (1995), thus setting the constant parameters which describe the relationship for PATNET stations. The following equation was derived:

$$M_L = 2.32 \text{ Log } (T) + 0.0013D + c \tag{8}$$

where T is the signal duration, D is the epicentral distance in km and c a constant different for each station. The constant c was calculated in a least-squares sense using 47 events which had been assigned local magnitude M_L by the National Observatory of Athens (NOA). Thus the above equation was calibrated at all PATNET stations for the local magnitude reported by the NOA.

We follow ZUCCA's *et al.* (1994) definition of pulse width on velocity seismograms as the time between the linear extrapolation of the rising slope at half peak, to the time axis and the first zero crossing (Fig. 2). A typical calibration of the complete system for the PAP station is shown in Figure 3. Judging from this figure we can see that frequencies of the initial portion of P wave analyzed are within the range of the "flat response" of the instrument.

4. The Patras Earthquake Sequence

The Patras earthquake sequence was well recorded by PATNET. The STALTA triggering technique was used in conjunction with continuous recording, enabling the recording of very small events down to magnitude 0.5 M_L.

The main shock in July 14, 1993 registered a magnitude of 5.4 M_s and was located at 38.19°N, 21.76°E with a focal depth of 5 km. The latter was confirmed by numerical modeling of strong motion recordings in the nearby city of Patras (TSELENTIS *et al.*, 1996). The main shock had a complex S-wave group mainly due to structural (path and site) effects. Discrete wavenumber and empirical Green's function methods used (TSELENTIS *et al.*, 1996; SOKOS *et al.*, 1997), suggested two

values of the source radius: $r = 1.9$ km and 3.0 km. The best fitting synthetics are obtained for $r = 1.9$ km. Although this source radius seems too small to produce the teleseismically observed corner frequency of 0.3 Hz, it cannot be ruled out, partly due to uncorrected structural complexities in the focal zone. If the latter is true, the stress drop is assessed as 20 MPa, i.e., higher than often reported for comparable events in W. Greece (MELIS *et al.*, 1995). Whatever the true source radius was, the ratio of the stress drops between the main shock and aftershocks was very high (31 and 17 for $r = 1.9$ and 3 km, respectively).

The scalar seismic moment is $M_0 = 3.2 \times 10^{17}$ NM. The Harvard double-couple focal mechanism solution of strike = 238°, dip = 73° and rake = −163° is assumed, because it is acceptable from the geological point of view. Together with the location, the focal mechanism suggests that the event was a manifestation of the recent activity of the Saravali fault (Fig. 4a).

The recorded aftershock sequence is depicted in Figure 4a and is divided in three clusters (cluster 1 is south, cluster 2 is central and cluster 3 is north) with a mean distance from the PAP station of 45 km, 40 km and 50 km, respectively.

Figures 4b and 4c depict the focal depth distribution of the hypocenters projected on a NW–SE and a SW–NE line, respectively. Thus, the NW–SE trending feature is followed and analyzed in space.

The first area of dispersed seismicity (southern part of cluster 1 and surroundings) is related to the numerous neotectonic faults of NE-SW direction. In the second area (cluster 2 and the northern part of cluster 1), the feature with a NW-SE trend direction lies at the junction where the Rio graben meets with the

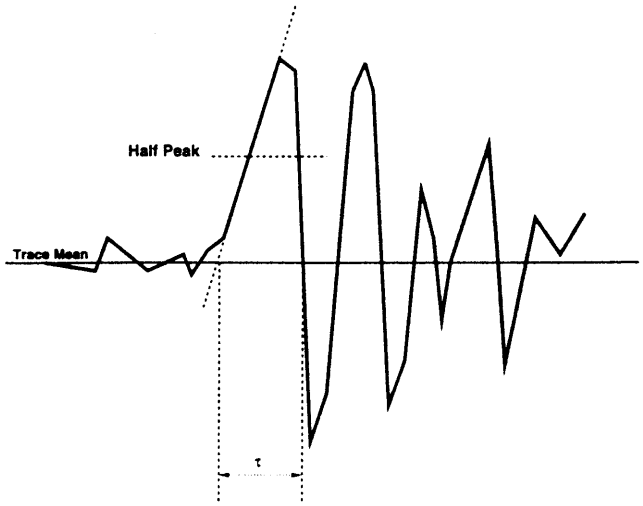

Figure 2
Definition of pulse width on velocity seismograms following ZUCCA *et al.* (1994).

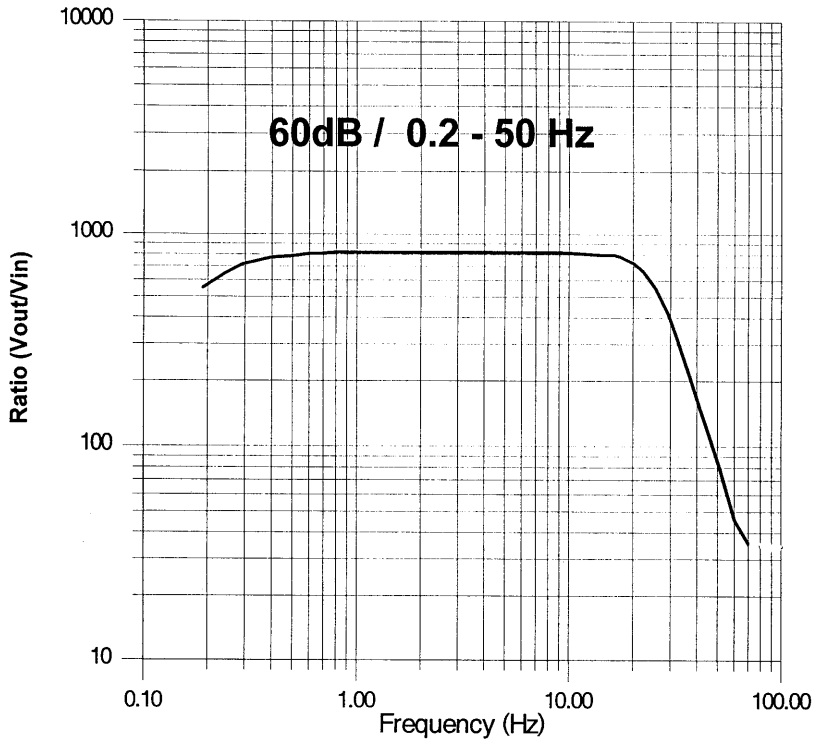

Figure 3
Calibration curve of PAP station.

Patras graben. It is interesting that the focal depths are concentrated at the range of 22 to 30 km, nearly forming a flat line approximately 35 km long. The third area (cluster 3) with the dispersed seismicity covers the Trichonis Lake and surroundings. Here, focal depths range from 3 to 20 km. This is also seen in other microearthquake studies in the area (PEDOTTI, 1988; MELIS, 1992).

The apparent alignment of the aftershocks does not imply the existence of a single fault (vertical to the Saravali fault) but signifies the activation of many parallel E–W trending small faults (TSELENTIS *et al.*, 1994).

5. Pulse Width Analysis and Results

In order to estimate the correction term $c(R)$ in eq. (7), the pulse width at station PAP was measured for very small aftershocks of all three clusters of the Patras aftershock sequence.

Figures 5a,b,c, display the frequency distribution of the pulse width measured for earthquakes with magnitude $M_L < 2.0$ R. Based on this result, the values of

$c = 0.065$ sec, $c = 0.04$ sec, and $c = 0.07$ sec, are adopted for the south, central and north clusters, respectively.

GLADWIN and STACEY (1974) and ZUCCA *et al.* (1994) demonstrated that the pulse width for an impulsive source is expressed by t/Q, where t is the travel time and Q is the quality factor describing the wave attenuation. Taking this into consideration we assessed an average first estimate of Q from the following formula

$$\bar{Q} = \frac{1}{nV_p} \sum_{i=1}^{n} \frac{R_i}{T_i}. \tag{9}$$

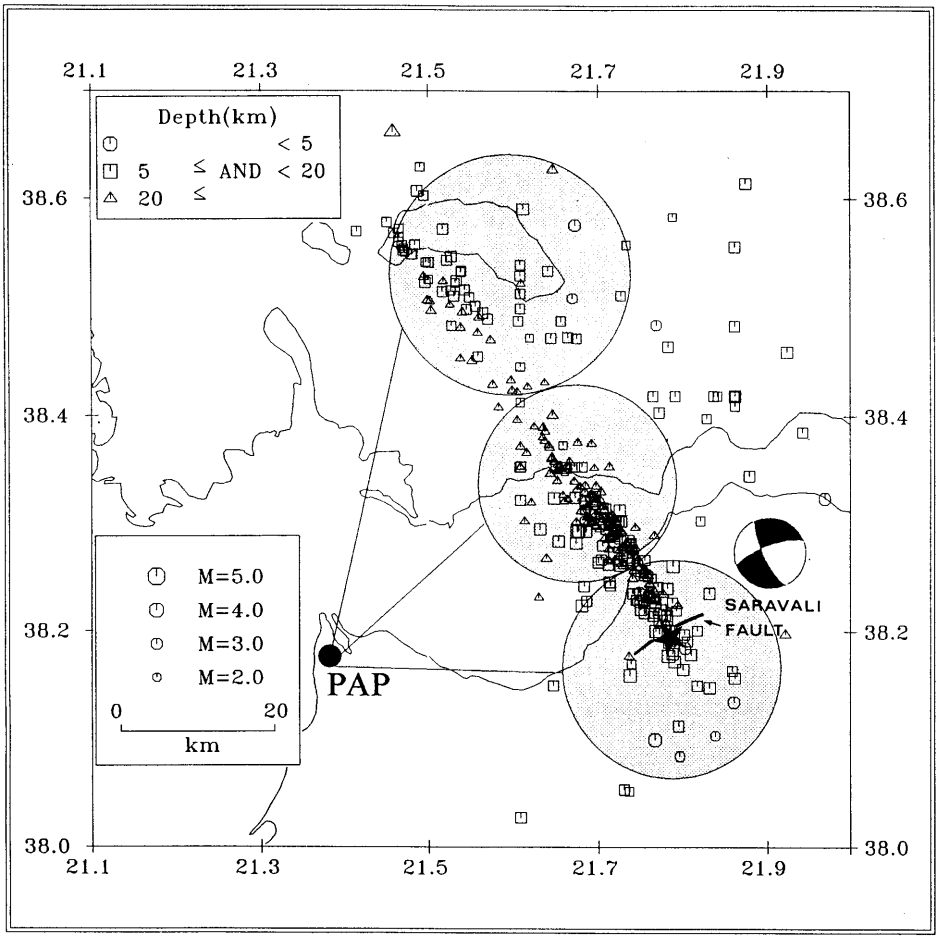

Figure 4(a)

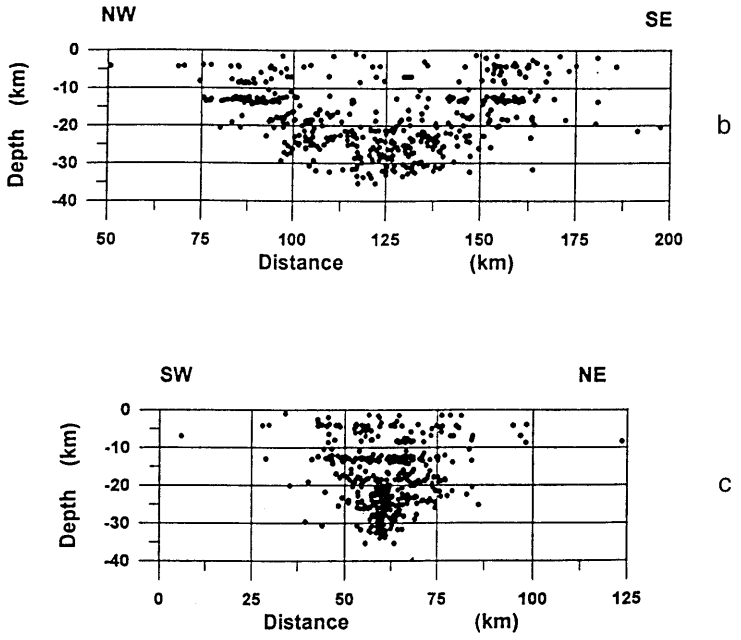

Figure 4
(a) Location of the aftershock clusters and the observation station PAP, the Saravali fault and fault plane solution are also depicted. (b,c) Depth cross section of hypocenters projected on NW–SE and SW–NE line, respectively.

From this relation we obtain an average value of $Q \cong 140$. This value for the crustal P wave is in good agreement with the results of TSELENTIS (1993, 1997).

To establish the empirical relation between the pulse width and earthquake local magnitude M_L, the pulse width of the initial P wave was read for all well located aftershocks of the three clusters of the Patras aftershock sequence.

Figures 6a,b,c, depict the obtained results in which the mean intrinsic pulse width T' $(= T_{\text{obs}} - c)$ is plotted against an earthquake magnitude for each cluster. By applying a linear curve to the whole data set we obtain the following regression curves

$$\begin{aligned} \log T' &= (0.36 \pm 0.14) M_L - 2.33 \pm 0.44 \quad \text{cluster 1} \\ \log T' &= (0.34 \pm 0.04) M_L - 1.97 \pm 0.12 \quad \text{cluster 2} \\ \log T' &= (0.76 \pm 0.09) M_L - 3.65 \pm 0.28 \quad \text{cluster 3} \end{aligned} \tag{10}$$

Combining eq. (6) with eq. (10) we can now establish the statistical relation between the earthquake magnitude M_L and fault length L (where $2T'$ is equalized to T) as

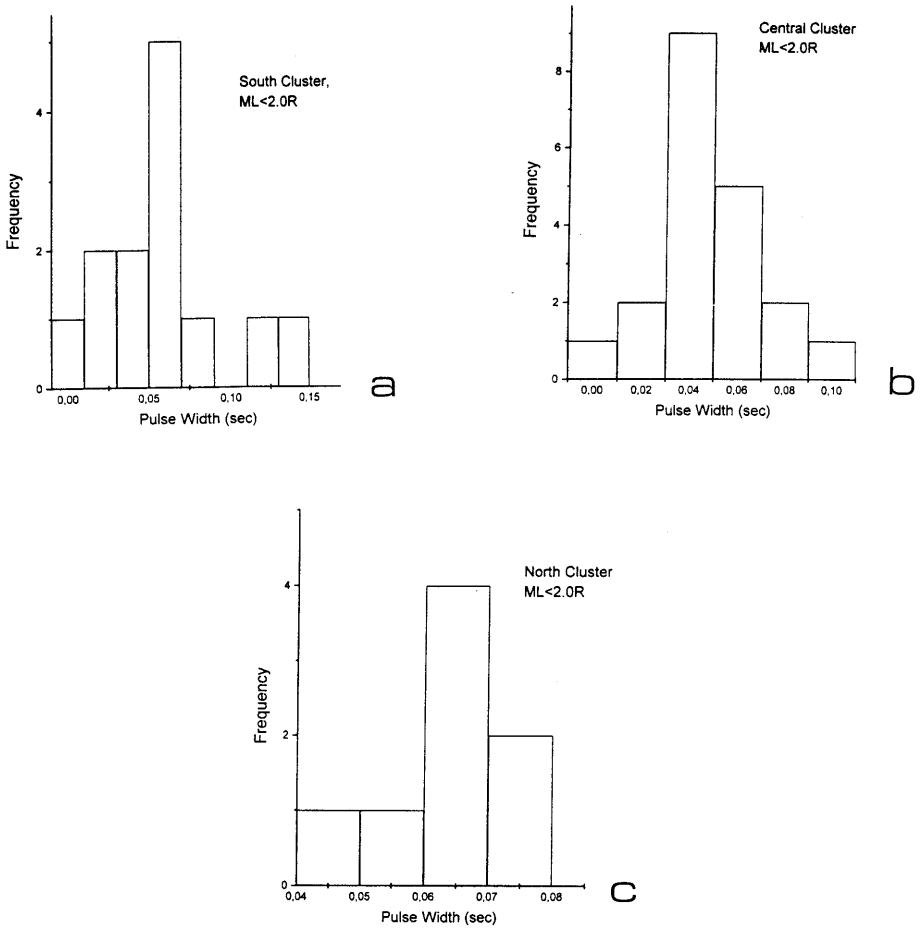

Figure 5
Frequency distribution of the pulse width for the aftershocks of magnitude less than 2.0 R for a) cluster 1, b) cluster 2 and c) cluster 3.

$$\begin{aligned} &\log L = 0.36M_L - 1.43 \quad \text{(circular crack)} \\ &\log L = 0.36M_L - 1.48 \quad \text{(bilateral fault)} \quad \text{cluster 1} \\ &\log L = 0.36M_L - 1.59 \quad \text{(unilateral fault)} \end{aligned} \tag{11a}$$

$$\begin{aligned} &\log L = 0.34M_L - 1.06 \quad \text{(circular crack)} \\ &\log L = 0.34M_L - 1.12 \quad \text{(bilateral fault)} \quad \text{cluster 2} \\ &\log L = 0.34M_L - 1.23 \quad \text{(unilateral fault)} \end{aligned} \tag{11b}$$

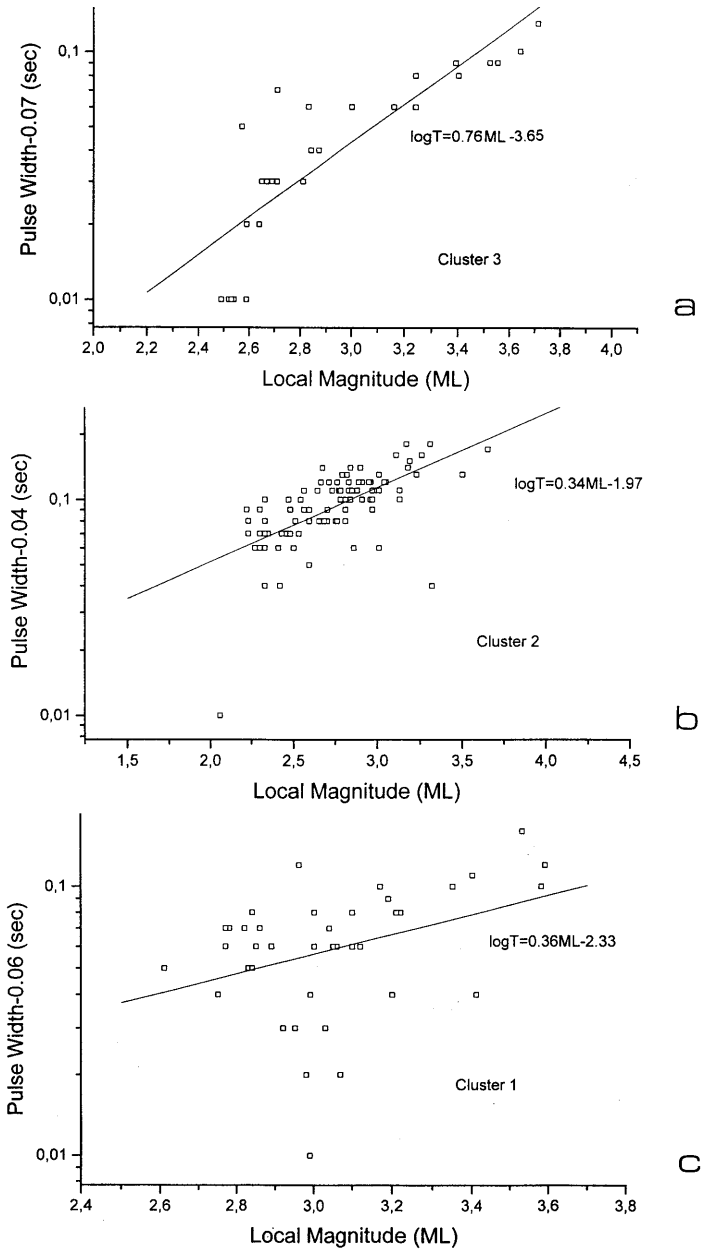

Figure 6
Relation between the intrinsic pulse width and local magnitude for a) cluster 1, b) cluster 2 and c) cluster 3.

$$\log L = 0.76M_L - 2.75 \quad \text{(circular crack)}$$
$$\log L = 0.76M_L - 2.79 \quad \text{(bilateral fault)} \quad \text{cluster 3} \tag{11c}$$
$$\log L = 0.76M_L - 2.90 \quad \text{(unilateral fault)}$$

All the above relations are presented in Figure 7. As is seen in the figure, events corresponding to clusters 1 and 2 manifest similar dependence between M_L and fault length L. This cannot be observed for the events of cluster 3 and possibly can be explained by the totally different tectonic regime of this region.

PAPAZACHOS (1989) proposed the following statistical correlation between fault length L and M_S

$$\log L = -1.85 \pm 0.51\ M_S. \tag{12}$$

Taking into consideration the recently published relation between M_L and M_S for the area of Greece (PAPAZACHOS *et al.*, 1997)

$$M_L = 0.58\ M_S + 2.14 (3.0 < M_S < 6.0) \tag{13}$$

we obtain

$$\log L = 0.87\ M_L - 2.94. \tag{14}$$

This relation is also depicted in Figure 6 and it seems to be in good agreement with the results of the present study (for the magnitude interval $2 < M_L < 4.0$ for which eq. (11) can be considered as valid).

MELIS (1992) examined the spectra of 94 microearthquakes in the region of the present investigation and proposed the following relations between seismic moment (M_0), local magnitude and circular source radius (r in m)

$$\log M_0 = 8.45 + 1.54\ M_L \tag{15}$$

$$\log M_0 = -2 + 7.28 \log r \tag{16}$$

from which we can derive the relation (assuming $L = 2r$)

$$\log L = 0.21\ M_L - 1.86 \quad \text{(in km)}. \tag{17}$$

This relation is also depicted in Figure 6 and it shows systematically lower L for magnitudes higher than 2.0 R.

By combining the relation between seismic moment and M_L (eq. 15) with eqs. (11a,b,c) corresponding to the circular crack, we obtain the following relations between seismic moment and source dimensions for clusters 1, 2 and 3, respectively.

$$M_0 = 9.12 \times 10^{14} L^{4.33} \tag{18a}$$

$$M_0 = 1.77 \times 10^{13} L^{4.52} \tag{18b}$$

$$M_0 = 1.58 \times 10^{14} L^{2.03}. \tag{18c}$$

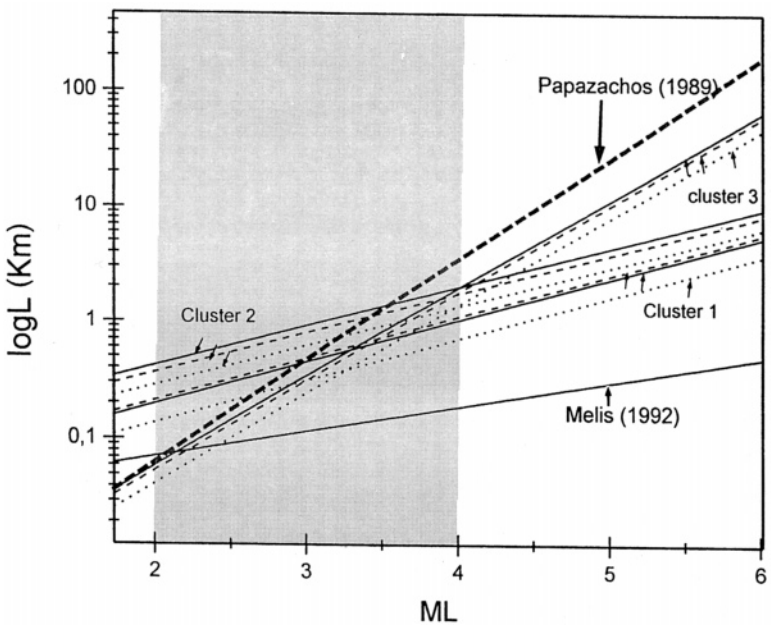

Figure 7
Relationships between the fault length and the local magnitude for the three clusters and three types of faulting (solid, dashed and dotted lines correspond to circular crack, bilateral and unilateral faults). The relations of PAPAZACHOS (1989) and MELIS (1992) are also plotted for comparison. Shaded area indicates the region of comparison.

If the similarity law among the fault length L, width W and displacement D is kept (KANAMORI and ANDERSON, 1975), M_0 should be proportional to L^3. As it is seen from the above relations, the exponent of L is less than 3 for cluster 3 and greater than 3 (and almost similar) for clusters 1 and 2, probably due to different tectonic regimes. This implies that the ratios W/L and/or D/L become larger for smaller earthquakes for cluster 3 and smaller for clusters 1 and 2.

6. *Conclusions*

This investigation demonstrates that the simple technique of initial P-wave pulse widths can be effective enough to provide reliable information of the seismic source of microearthquake data. By using this approach, we established the statistical relation between the fault length and local earthquake magnitude of the aftershock sequence of the Patras July 1993 earthquake. Furthermore, the relation between seismic moment and fault length was also established. The results were compared

with other published relations and revealed that the ratios of fault width and/or displacement to length were greater for cluster 3 and smaller for clusters 1 and 2 which could be explained by the different tectonics of the regions covered by clusters 1, 2 and 3, respectively.

Acknowledgements

I am grateful to Drs. N. Melis, P. Burton, J. Zahradnik, T. Sokos and an anonymous reviewer for their most useful suggestions.

References

Brune, J. N. (1970), *Tectonic Stress and the Spectra of Seismic Shear Waves from Earthquakes*, J. Geophys. Res. *75*, 4997–5009.

Frankel, A. (1981), *Source Parameters and Scaling Relationships of Small Earthquakes in the North-eastern Caribbean*, Bull. Seismol. Soc. Am. *71*, 1173–1190.

Frankel, A., and Kanamori, H. (1983), *Determination of Rupture Duration and Stress Drop for Earthquakes in Southern California*, Bull. Seismol. Soc. Am. *73*, 1527–1551.

Gladwin, M. T., and Stacey, F. D. (1974), *Anelastic Degradation of Acoustic Pulses in Rock*, Phys. Earth Planet. Inter. *8*, 332–336.

Lee, W. H. K., Bennet, R. E., and Meagher, K. L. (1972), *A Method of Estimating Magnitude of Local Earthquakes from Signal Duration*, USGA Open File Report, 1–28.

Lee, W. H. K., and Valdes, C. M. (1985), *HYPO71PC: A Personal Computer Version of the HYPO71 Earthquake Location Program*, USGS Open File Report, 1–28.

Melis, N. S. (1992), *Earthquake Hazard and Crustal Deformation in Central Greece*, Ph.D. Thesis, University of Wales, UK.

Melis, N. S., Burton, P. W., and Brooks, M. (1995), *Coseismic Crustal Deformation from Microseismicity in the Patras Area*, Geophys. J. Int. *122*, 815–836.

Ohtake, M. (1986), *Fault Length of Small Sized Earthquakes as Estimated from the Pulse Width of Initial P Wave*, J. Phys. Earth *34*, 397–406.

O'Neill, M. E., and Healy, J. H. (1973), *Determination of Source Parameters of Small Earthquakes from P-wave Rise Time*, Bull. Seismol. Soc. Am. *63*, 599–614.

O'Neill, M. E. (1984), *Source Dimensions and Stress Drops of Small Earthquakes near Parkfield, California*, Bull. Seismol. Soc. Am. *74* (1), 22–40.

Papazachos, B. C., Kiratzi, A. A., and Karacostas, B. G. (1997), *Toward a Homogeneous Moment-magnitude Determination for Earthquakes in Greece and the Surrounding Area*, Bull. Seismol. Soc. Am. *87* (2), 474–483.

Pedotti, G. (1988), *Etude sismotectonique du Peloponnese et response sismique d'une valle sedimentaire en Grece du Nord*, Thèse, Université Joseph Fourier, Grenoble.

Sokos, E., Tselentis, G.-A., Plicka, V., and Zahradnik, J. (1987), *An Attempt to Explain Strong Motion Records of Patras 93 Earthquake*, IASPEI, Abstracts, p. 333.

Tselentis, G.-A., Makropoulos, K., and Voulgaris, N. (1989), *Cluster and Spectral Characteristics of the Aftershock Activity of the Kalamata, September 13, 1986 Earthquake, S. Greece*, Tectonophysics *169*, 135–148.

Tselentis, G.-A. (1993), *Depth Dependent Seismic Attenuation in W. Greece*, Tectonophysics *225*, 523–528.

Tselentis, G.-A., Xanalatos, N., and Melis, N. S. (1994), *SISMWIN: A Computer Program for Seismological Data Phase Picking and Processing*, Report C2, Patras Seismological Centre, 76pp.

TSELENTIS, G.-A., MELIS, N. S., and SOKOS, E. (1994), *The Patras (July 1993) Earthquake Sequence as it was Recorded by the Patras Seismic Network*, Proc. Conf. Geol. Soc. Greece, Thessaloniki.

TSELENTIS, G.-A., KOUKIS, G., SOKOS, E., RUBAS, D., JANSKY, J., PLICKA, V., PAKZAD, M., and ZAHRADNIK, J. (1996), *Modelling the Strong Ground Motions in the City of Patras*, *Greece*, *during July 1993 Earthquake*, Proc. Eleventh WCEE, Acapulco, Mexico, vol. 1, pp. 238–246.

TSELENTIS, G.-A. (1997), *Intrinsic and Scattering Seismic Attenuation in W. Greece*, Pure appl. geophys., in press.

WU, H., and LEES, J. (1996), *Attenuation Structure of Coso Geothermal Area*, *California*, *from Wave Pulse Widths*, Bull. Seismol. Soc. Am. *86* (5), 1574–1590.

ZUCCA, J. J., HUTCHINGS, L. J., and KASAMEYER, P. W. (1994), *Seismic Velocity and Attenuation Structure of the Geysers Geothermal Field*, *California*, Geothermics *23*, 111–126.

(Received June 16, 1997, accepted October 18, 1997)